Confirmation of the Existence of Modulation Wave Motion in Incommensurate Rb_2ZnCl_4 by Hahn Echo and 2D NMR

Ligia Muntean, Ursa Mikac[a], R. K. Subramanian[b], and David C. Ailion[c]

JILA, Campus Box 440, University of Colorado, Boulder, CO 80309, USA
[a] J. Stefan Institute, Ljubljana, Slovenia
[b] Microcosm Inc., 4130 Guilford Road, Suite O, Columbia, MD 21046, USA
[c] Dept. of Physics,University of Utah,115 South 1400 East, Salt Lake City, Utah 84112, USA

Reprint requests to Prof. D. C. A.; Email: ailion@physics.utah.edu

Z. Naturforsch. **57 a,** 353–362 (2002); received January 25, 2002

Presented at the XVIth International Symposium on Nuclear Quadrupole Interactions, Hiroshima, Japan, September 9-14, 2001.

^{87}Rb Hahn echo nuclear magnetic resonance (NMR) and ^{35}Cl Hahn echo nuclear quadrupole resonance (NQR) measurements were performed at 293 - 302 K in the incommensurate (I) phase of Rb_2ZnCl_4. The existence of a Hahn echo decay that is shorter than the true T_2 and one that has an exponential dependence on the cube of the echo time indicates the presence of slow motions. The diffusion coefficient D can be obtained from the rate of decay of the Hahn echo. Similar values for D were obtained from the two different measurements, indicating that both the Rb and the Cl atoms are experiencing the same motional mechanism. This mechanism must be due to simultaneous motions of each and can not be due to individual motions of only one type of atom. Further confirmation of the presence of modulation wave motion was obtained from ^{87}Rb two-dimensional (2D) exchange-difference NMR measurements.

Key words: Incommensurate; Modulation Wave; Hahn Echo; 2D Exchange NMR.

1. Introduction

Considerable interest in recent years has been focused on understanding the properties of incommensurate (I) systems [1, 2]. These systems have at least two competing periodicities [that of the incommensurate modulation wave (or waves) and that of the underlying crystal structure] whose wave vectors are not rational multiples of one another. Thus, they exhibit long range order but no translational symmetry and, hence, can be regarded as intermediate between perfect crystals and glasses.

Nuclear magnetic resonance (NMR) and nuclear quadrupole resonance (NQR) have proven to be powerful techniques for elucidating the static and dynamic properties of the modulation wave in the I state. The static properties have been studied primarily by lineshape measurements [3 - 5] and the dynamic properties (i. e., those involving amplitudon and phason dynamics as well as diffusion-like motions of the modulation wave) by relaxation time [6 - 10], Hahn spin-echo magnetization decay [11 - 13], and two-dimensional (2D) exchange NMR [14 - 16] studies.

An ideal impurity-free I system is characterized by the existence of a gapless phason (Goldstone) mode in which the I modulation wave moves through the crystal without friction [1, 2]. This theoretical prediction, based on the fact that the Gibbs free energy is independent of the phase of the modulation, has not been directly observed in real I systems which have discrete structure and impurities that pin the modulation wave [2]. Due to thermal fluctuations, the pinning potential can be overcome so that the modulation wave can become temporarily depinned and mobile. Since the pinning centers have a random spatial distribution and pinning strength, the thermal depinning is random, giving rise to a random diffusion-like character of the modulation wave motion [11, 12].

Normally, slow diffusion of an observed spin in an inhomogeneous magnetic field can result in the decay of a Hahn echo (i. e., following a 180°-90° sequence) being more rapid than that of a Carr-Purcell-

Meiboom-Gill (CPMG) decay [17]. Furthermore, for free non-restricted diffusion the Hahn echo decay is usually characterized by an exponential dependence on the cube of the echo time τ. However, such behavior has recently been observed for quadrupolar systems in which the magnetic field is homogeneous [11 - 13] and in which the observed spin may be stationary [11]. These observations were attributed to a spatially inhomogeneous electric field gradient (EFG) which fluctuates in time due to the diffusion-like motions of the incommensurate modulation wave between the pinning centers. (A similarly short Hahn-echo decay time has also been observed in other systems, characterized by different fluctuating interactions (e. g., Knight shift [18] and chemical shift [19]), and attributed to slow atomic or molecular motions.) However, in the case of Rb_2ZnCl_4, observation of a rapid ^{35}Cl NQR Hahn decay with an exponential dependence on τ^3 does not unambiguously prove the existence of modulation wave motions because of the possibility that these results may simply reflect slow reorientations of the $ZnCl_4$ tetrahedra. A primary purpose of this paper is to present data which unambiguously demonstrate in Rb_2ZnCl_4 that slow modulation wave motions are responsible for the rapid ^{35}Cl NQR Hahn echo decay observed previously [12, 13].

In this paper we describe two approaches for investigating slow diffusion of the I modulation wave in Rb_2ZnCl_4: 1) measurement of the rapid decays of both the ^{87}Rb NMR and the ^{35}Cl NQR Hahn spin echo amplitudes arising from EFG fluctuations and 2) measurement of the cross peak displacement in a ^{87}Rb 2D exchange-difference NMR experiment. Those data provide conclusive evidence for the existence of the modulation wave motion.

It is well known [20] that Rb_2ZnCl_4 undergoes two successive phase transitions, a paraelectric-incommensurate transition at $T_I \cong 302$ K and an incommensurate-commensurate transition at $T_C \cong 192$ K. The high temperature paraelectric (P) phase belongs to the orthorhombic space group P_{cmn}-$D_{26}{}^{16}$ (No. 62) with four formula units per unit cell. The low temperature commensurate (C) phase, $C_{2v}{}^9$, is ferroelectric. In the ferroelectric phase the lattice parameter is tripled along the pseudohexagonal c axis [1].

The P unit cell contains eight Rb ions which can be divided into chemically inequivalent sets, Rb(1) and Rb(2). The Rb(1) sites lie on the pseudohexagonal and the Rb(2) sites on the pseudotriad axes [21]. All Rb sites have mirror symmetry and lie in the mirror plane perpendicular to the crystal b axis. Due to the presence of the center of symmetry, at most two Rb sites can be distinguished for each chemically inequivalent set. It is thus expected that we would see at most four Rb lines for $T > T_I$. For an arbitrary direction of the magnetic field in either the ab or cb planes, the two lines of each inequivalent set coincide because of symmetry [22]. For $a \perp H_0$, only one ^{87}Rb NMR line should be observed for each inequivalent set.

2. Experimental Details

The ^{87}Rb NMR experiments were performed on a Rb_2ZnCl_4 single crystal by irradiating at 116.15 MHz the central transition, 1/2→–1/2. The crystal was oriented such that $a \perp H_0$ and $\angle c, H_0 = 120°$.

The Hahn spin-echo magnetization decay was measured with the $\pi/2$-τ-π-τ-echo sequence, and the corresponding spin-spin relaxation time T_2 was obtained with the standard CPMG technique. For all pulse sequences the phase cycling includes the Cyclops quadrature-error compensation scheme [23]. The 2D exchange-difference technique [14] will be described in detail in the next Section.

Temperature control and variation was achieved by an Oxford cryogenic system, such that the temperature stability was ± 0.1 K at all temperatures studied. The pulse sequence generation, acquisition, and analysis were performed using a TecMag-Aries NMR system.

3. 2D Exchange-difference NMR

The 2D exchange-difference NMR technique [14, 24] is a variant of the 2D exchange NMR technique [24] involving taking the difference between 2D exchange NMR signals at two different mixing times, one long and one as short as possible. The standard 2D exchange NMR technique can in principle detect any spatial motion of the resonant nucleus during the mixing time t_{mix} such that the Larmor frequencies at the beginning and the end of t_{mix} are different, and is most useful for studying dynamic processes which are too slow to affect the lineshape. The 2D spectrum $S(\nu_1, \nu_2)$ is a plot of the NMR intensity vs. two frequencies, ν_1 and ν_2, whose values correspond, respectively, to the initial and final Larmor frequencies of the moving spins. Static nuclei with resonance frequencies that are unchanged during t_{mix} contribute to the diagonal intensity ($|\nu_1| = |\nu_2|$). Nuclei which jump during t_{mix} to other lattice sites where they have

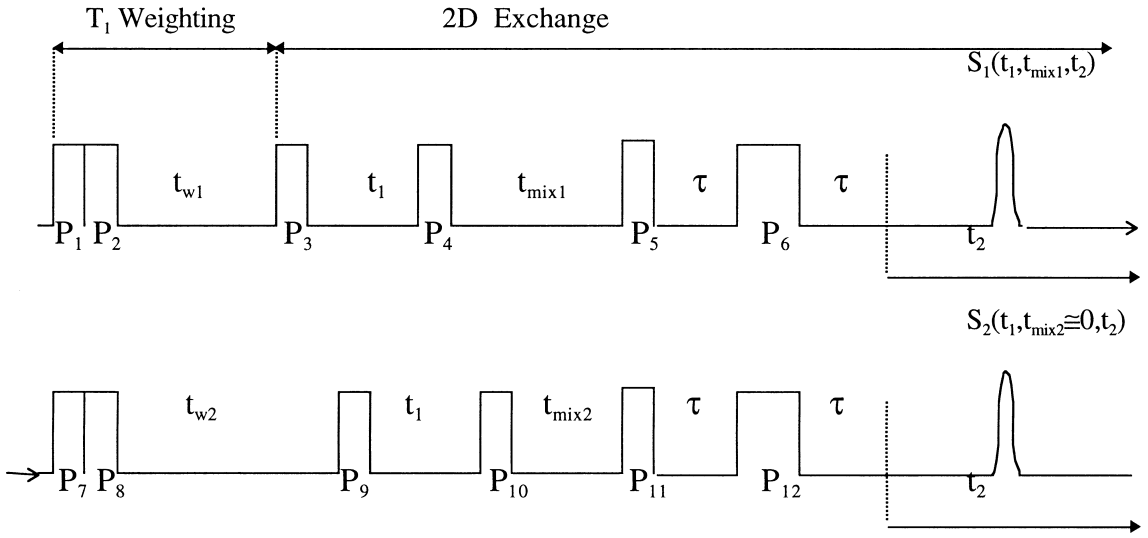

Fig. 1. 2D exchange - difference NMR pulse sequence.

different resonance frequencies, however, create off-diagonal ($|\nu_1| \neq |\nu_2|$) peaks, called cross peaks. The diagonal portion of the 2D spectrum is continuous in the case of inhomogeneously broadened spectra (such as for I systems); its length is a measure of the inhomogeneous broadening, and its width corresponds to the homogeneous linewidth originating from T_2 processes. The standard 2D exchange NMR method is not applicable to such situations where the frequency change due to motions is very small compared to the width of the continuous diagonal. In this case cross peaks will not be resolved from the continuous diagonal and, hence, can not be observed or identified. The solution to this problem is to apply the 2D exchange-difference NMR technique [14, 24].

In 2D exchange-difference NMR, static spins on the diagonal are eliminated from the 2D exchange-difference spectrum by subtraction, since they give the same signal, independent of the length of the mixing time. Hence, the 2D exchange-difference spectrum arises from only moving spins. Because some spins have moved from the diagonal to the cross peaks during the mixing time t_{mix}, the diagonal of the difference spectrum will have a negative intensity and will contrast to the cross peaks which have a positive intensity. In this way, those spins which moved during t_{mix} (and are responsible for the cross-peak signal) can be easily distinguished from the static spins (that had been on the continuous diagonal before the subtraction).

The pulse sequence [14, 25] is presented in Figure 1. The 2D exchange part consists of four pulses (P_3, P_4, P_5, P_6) for the first sequence and four more pulses (P_9, P_{10}, P_{11}, P_{12}) for the second. The first three pulses of each sequence (P_3, P_4, P_5 and P_9, P_{10}, P_{11}) are 90° pulses and form the basic 2D exchange sequence that produces a stimulated echo at a time t_1 after the third 90° pulse. The role of the 180° pulses in Fig. 1 (P_6 and P_{12}) is to push the echo out by an extra time τ, so that ringdown effects are avoided for short t_1's. The phase-cycling scheme is given in [14, 25].

The two 2D exchange signals are affected differently by the spin-lattice relaxation due to the fact that the two mixing times are different. In order to obtain accurate information about the exchange process from the 2D exchange-difference spectrum, T_1 weighting of both 2D exchange signals has to be the same. For this reason, two additional T_1-weighting intervals t_{w1} and t_{w2} have been applied prior to the exchange parts of the sequence, as described below. The first two pulses in Fig. 1 form a composite pulse which is cycled between 0° (90_{x} followed by 90_{-x}) and 180° (90_x followed by 90_x). The 0° composite pulse could in principle have been omitted, but it is kept as a reminder of the procedure. At the end of the t_{w1} period following the 0° and 180° composite pulses, the z magnetizations are $M_{\mathrm{z}}(t_{\mathrm{w1}}) = M_0$ and $M_{\mathrm{z}}(t_{\mathrm{w1}}) = \mathrm{M}_0[1 - 2\exp(-t_{\mathrm{w1}}/T_1)]$, respectively. The subtraction of these M_{z} components yields

the T_1-weighted magnetization, $M_z(t_{w1}) = 2\ M_0 \exp[-t_{w1}/T_1]$, at the beginning of the exchange part of the sequence. At the end of the first 2D exchange sequence the amplitude of the signal is T_1 weighted with a factor $\exp[-(t_{w1} + t_{mix1})/T_1]$ and, similarly, at the end of the second 2D exchange sequence with a factor $\exp[-(t_{w2} + t_{mix2})/T_1]$. By setting $t_{w1} + t_{mix1} = t_{w2} + t_{mix2}$, we have arranged that spin-lattice relaxation will affect equally the amplitudes of the signals in both 2D exchange sequences. In this way, the 2D difference spectrum will reflect only the exchange process even for long mixing times (3 T_1 or longer). This subtraction is performed in the computer by changing the sign of the receiver phase in two consecutive scans.

The two 2D exchange parts preceded by the corresponding T_1-weighting sections can be viewed as a single sequence even though they are separated by the repetition time of the whole sequence. Signal acquisition occurs twice in the entire sequence.

The phase cycling, consisting of 64 steps, has been designed for the central transition of any noninteger spin ($I > 1/2$) for which inhomogeneous broadening is produced by the second order electric quadrupolar interaction. When only the central transition, $1/2 \rightarrow -1/2$, is irradiated, the problem is mathematically equivalent to that of a system of uncoupled $I = 1/2$ spins. We used the "real Fourier transformation (FT) in t_1" method [24] to obtain pure absorption 2D spectra. This technique involves a real FT in the t_1 time domain and a complex FT in the t_2 time domain of a signal that is amplitude modulated with a cosine function in t_1 but is complex in t_2. In summary, our phase cycling scheme results in pure 2D absorption spectra in which T_1 effects are eliminated and baseline and quadrature errors are compensated (via the Cyclops scheme).

4. Results and Discussions

4.1. Hahn Spin-echo Magnetization Decay Results

The Hahn spin-echo magnetization decay in a spatially inhomogeneous EFG has provided a way to measure in I systems extremely small diffusion coefficients (in the range 10^{-12} - 10^{-15} cm^2/s) [11 - 13]. The physical explanation of this high sensitivity is that the modulation wave in an I solid produces a much larger frequency variation over much smaller distances than is obtainable by the conventional magnetic field gradient technique. The presence of diffusion is inferred from:(1) the Hahn spin-echo decay being shorter than the CPMG echo decay, and 2) the Hahn spin-echo magnetization having an exponential dependence on the cube of the echo time. The spatially varying EFG is a characteristic feature of any quadrupolar system that lacks translational symmetry. A necessary condition for the determination of the diffusion coefficient is knowing the spatial variation of the intrinsic EFG, which then provides a known relationship between position and NMR frequency.

This new approach to interpreting the Hahn spin echo data was first applied in incommensurate Rb_2ZnCl_4 by NQR measurements of ^{35}Cl [12, 13]. However, a short Hahn spin-echo decay can, in some systems, be due to several possible motional mechanisms [26] that cannot be easily distinguished from one another just by observation of a more rapid Hahn echo decay. For example, observations in Rb_2ZnCl_4 of a rapid ^{35}Cl NQR Hahn decay having an exponential dependence on τ^3 do not unambiguously prove the existence of modulation wave motion because such results could alternatively have arisen simply from slow reorientations of $ZnCl_4$ groups between two sites.

One method of proving the existence of modulation wave motion is to measure the diffusion coefficient by using ^{87}Rb NMR and also by ^{35}Cl NQR and then to compare their values. In Rb_2ZnCl_4, the modulation wave is thought to originate from progressive misorientations of $ZnCl_4$ tetrahedra and corresponding small displacements of Rb atoms. The modulation wave motion, which is a collective motion that involves a large number of atoms, should thus affect both Rb and Cl ions comparably. Thus, observation of comparable values for diffusion coefficients obtained by ^{87}Rb NMR and ^{35}Cl NQR would strongly support the existence of the modulation wave diffusion.

The ^{87}Rb NMR spectra obtained at the same crystal orientation ($a \perp H_0$) over the temperature range 293 - 302.3 K are shown in Figure 2. When the temperature is lowered through the transition temperature T_I ($\cong$ 302 K), the Rb ions and the $ZnCl_4$ groups become displaced in the direction of the b axis and the $ZnCl_4$ tetrahedra are rotated around the c axis [22]. The incommensurate effects are clearly observed in the low frequency NMR line corresponding to Rb(2) nuclei, but they do not appear in the Rb(1) lineshape. The explanation for this fact is that the EFG tensor at the Rb(2) site is more strongly affected by the P-I transition than is the EFG tensor at the Rb(1) site

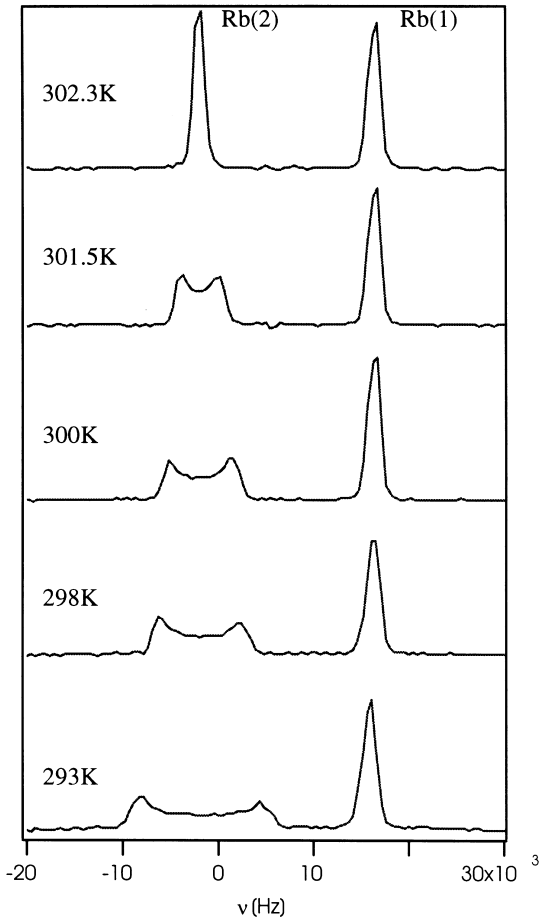

Fig. 2. ^{87}Rb NMR lineshapes in Rb_2ZnCl_4 in the temperature range 293 - 302.3 K.

[22], which suggests that Rb(2) has a larger displacement due to the I modulation wave amplitude than does Rb(1).

The Hahn spin echo decay was observed to be shorter than the CPMG echo decay (see Fig. 3) over the entire temperature range (293-302.6K). Furthermore, it has an exponential dependence on the cube of the echo time, whereas the CPMG decay varies exponentially with an exponent that is linear in the echo time and proportional to $1/T_2$.

For a linear frequency-space relation where $\omega(x) = \omega_0 + \omega_1 \sin(qx)$, which is valid for our specific crystal orientation ($a \perp H_0$), the decay of the transverse magnetization in a Hahn spin - echo experiment [11 - 13] is given by

$$M(2\tau) = M_0 \exp\left[-\frac{2\tau}{T_2}\right] \exp\left[-D_\omega \cdot (\omega_1 q)^2 \frac{2\tau^3}{3}\right]. \quad (1)$$

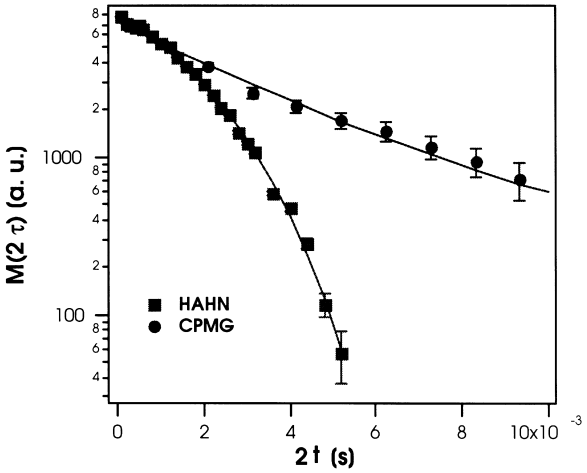

Fig. 3. ^{87}Rb NMR ■ Hahn and ● CPMG echo decays in the incommensurate phase of Rb_2ZnCl_4 at T = 299 K.

Here, ω_0 is the NMR angular frequency in the high temperature P phase and ω_1 is one half the distance between the edge singularities (at $\omega = \omega_0 \pm \omega_1$). D_ω is an apparent diffusion coefficient that is defined as $D_\omega = D \cdot \left[1 - \left((\omega - \omega_0)/\omega_1\right)^2\right]$, where D is the true diffusion coefficient.

D_ω thus depends on the position within the inhomogeneously broadened lineshape. The above theory [11 - 13] predicts that, for a diffusion length that is small compared to the wavelength of the modulation wave, D_ω is maximum and equals D at the center of the I lineshape (where the frequency gradient is a maximum) but has a minimum value (theoretically zero) at the edge singularities ($\omega = \omega_0 \pm \omega$) where the frequency gradient is zero. In this regime, where the modulation wave travels a distance short compared to its wavelength, the theoretical value of $D_\omega^{\mathrm{Max}}/D_\omega^{\mathrm{Min}}$ would be infinite, but should decrease when the diffusion occurs on a larger spatial scale. This decrease is due to the fact that, for long range modulation wave motion, each nucleus will then have sampled all displacements resulting in an averaged diffusion coefficient. This averaging should be equivalent to averaging over the I line and will be more pronounced for large scale modulation wave motion than for small scale motion.

We determined D_ω from a fit to (1) of the Hahn spin-echo magnetization decay curves (measured from the spectra). For each Hahn decay, a value for T_2 was obtained from CPMG measurements at the same frequency within the I lineshape.

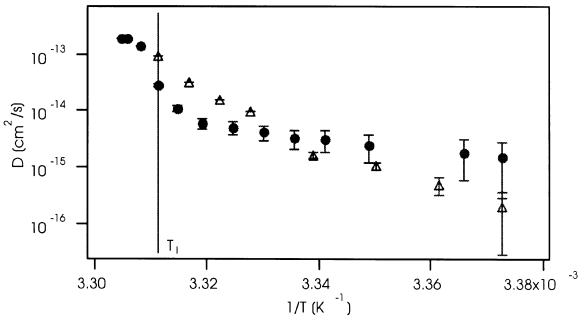

Fig. 4. The temperature variation of the diffusion coefficient obtained from ● ^{87}Rb NMR and Δ ^{35}Cl NQR.

Although the average diffusion of the modulation wave occurs on a short spatial scale in Rb_2ZnCl_4 in the investigated temperature range [14, 16], the ^{87}Rb Hahn spin echo data do not show an appreciable variation of D_ω across the I lineshape (the measured value of $D_\omega^{Max}/D_\omega^{Min} \cong 1.2$). In addition, the maximum value D_ω^{Max} does not appear at the center of the I lineshape but is shifted towards one of the singularities. We do not at present have an explanation for these discrepancies, but they may be due to theoretical approximations used in deriving (1), such as the linear approximation in the "frequency-space" relation and the local approximation [2]. The local approximation is valid when the dominant contribution to the EFG at a given spin comes from a region of radius much smaller than the modulation wave wavelength. The type of frequency-space relation used (linear, quadratic, or mixed linear-quadratic) depends on the orientation of the nuclear EFG tensor with respect to the external magnetic field. In our data analysis, we assumed that the maximum value D_ω^{Max} (obtained near the high frequency edge singularity) equals the true diffusion coefficient D.

We also performed ^{35}Cl NQR Hahn spin-echo magnetization decay measurements and obtained results similar to those published by Papavassiliou et al. [13]. The temperature variation of the diffusion coefficient obtained from our ^{87}Rb NMR and ^{35}Cl NQR Hahn-echo data is shown in Figure 4. As can be seen, the values of the diffusion coefficients are of comparable magnitude within experimental errors, especially in the high temperature region of the I phase. This fact strongly supports the existence of the slow diffusion-like motion of the modulation wave since such motion is a collective motion that should affect both Rb and Cl ions comparably. Jumps involving only Cl ions (e. g., reorientation of the $ZnCl_4$ tetrahedra without corresponding Rb motions) can be ruled out since such motions would give very different values for D measured by ^{87}Rb NMR and ^{35}Cl NQR.

We observed that the small discrepancies in the values of D obtained from ^{87}Rb NMR and from ^{35}Cl NQR increase as the temperature is lowered in the I phase (Fig. 4). This may be due to the fact that different samples, possibly having different impurity concentrations, were used in the ^{87}Rb NMR and ^{35}Cl NQR experiments. The modulation wave diffusion is likely to be affected by impurity pinning [14]. Such pinning depends on the impurity concentration and should have a greater inhibiting effect on modulation wave motion at lower temperatures.

The diffusion coefficient was observed to increase with increasing temperature, in agreement with previous reports [13, 26] on thermally activated modulation wave motion. Fast diffusion close to the transition temperature T_I probably originates from thermal depinning of the modulation wave. An interesting result of the Hahn spin echo decay measurements is that the maximum value of the diffusion coefficient D is obtained 0.5 K above the temperature at which the incommensurate NMR line broadening first becomes observable below the P-I transition. This can be explained by the fact that floating of the depinned modulation wave very close to T_I averages out the small I splitting of the lineshape [27].

4.2. ^{87}Rb 2D Exchange-difference NMR Results

We applied the 2D exchange-difference technique to study ultraslow motions in both the incommensurate and the high temperature paraelectric phases of Rb_2ZnCl_4. This dynamical study has proved to be useful in elucidating the nature of the I-P transition [16].

In the I phase we performed 2D exchange-difference experiments at five different temperatures in the interval 296.0 - 301.6 K. The highest temperature is very close to the I-P transition. The ^{87}Rb NMR absorption line is inhomogeneously broadened due to the second-order quadrupole interaction and has a width of approximately 11 kHz at T = 296 K. The 2D exchange-difference spectrum has a diagonal shape since the change in frequency during the mixing time is much smaller than the width of the inhomogeneous 1D spectrum. Figure 5 displays the ^{87}Rb 2D exchange-difference spectrum for part of the I lineshape (specifically, the part that includes the

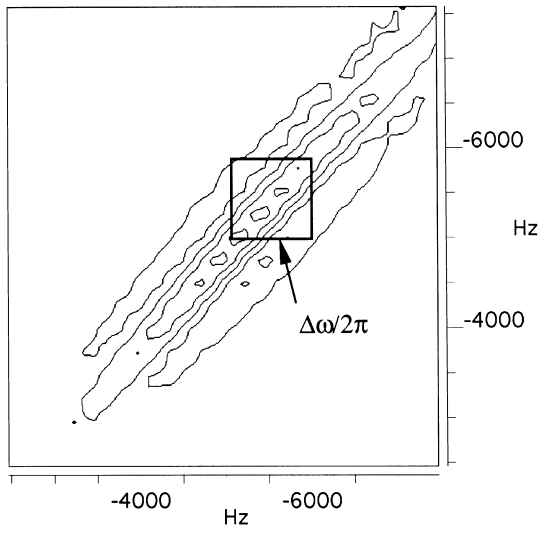

Fig. 5. ^{87}Rb 2D exchange - difference spectrum for part of the I lineshape (the edge singularity closest to the excitation frequency) at T = 296.0 K for t_{mix} = 4 ms. Reprinted with permission from [16].

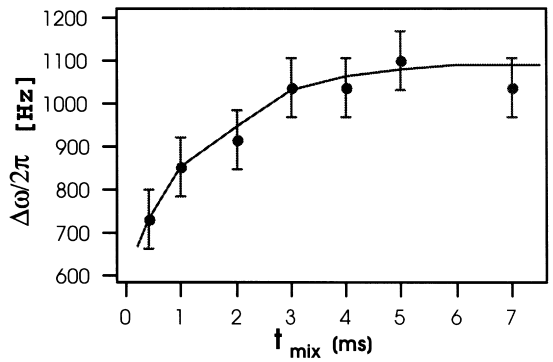

Fig. 6. The maximum change in the NMR frequency, $\Delta\omega/2\pi$, due to the motion of the modulation wave, plotted as a function of the mixing time, t_{mix} at T = 296.0 K. Reprinted with permission from [16].

edge singularity closest to the excitation frequency). The change in frequency due to motions is measured as the horizontal (or vertical) distance from the diagonal to the cross peaks (Fig. 5). The frequency shift of the cross peaks relative to the diagonal in the 2D exchange-difference spectrum is proportional to the average displacement of the modulation wave.

Figure 6 shows the results of experiments in which we increased the mixing time t_{mix} until an asymptotic value of the frequency shift was obtained. This asymptotic value of $\Delta\omega$ corresponds to the maximum distance traveled by the modulation wave. Note the continuous variation of the frequency shift with the mixing time. This continuous variation corresponds to the progressive motion of the modulation wave, which moves only a very small fraction of its wavelength in each step. This observation effectively rules out many alternative models for motions in this phase (e. g., random fluctuations due to two-site motions, librational oscillations, phason or amplitudon oscillatory motions, etc.). Such motions would not give rise to the observed progressive displacements and would likely be too rapid to be observed in our 2D spectra.

The modulation wave displacement can easily be obtained from the cross-peak frequency shift in the 2D exchange-difference spectrum. As mentioned earlier, for our crystal orientation ($a \perp H_0$) the NMR frequency has a linear dependence on the modulation wave amplitude [2] given by $\omega(x) = \omega_0 + \omega_1 \sin(kx)$. Here, k is the modulation wave vector, $\omega_0/2\pi$ is the NMR frequency at the center of the I spectrum, and ω_1 is proportional to the modulation wave amplitude and corresponds to half the linewidth of the I spectrum. The maximum modulation wave displacement X_{max} can then be determined from the asymptotic value of the measured frequency shift $\Delta\omega_{\mathrm{max}}/2\pi$ using the formula (derived in the Appendix),

$$X_{\mathrm{max}} = \frac{\lambda}{2\pi}\Big[\arcsin\Big(\frac{\Delta\omega_{\mathrm{max}} + \omega(x) - \omega_0}{\omega_1}\Big) - \arcsin\Big(\frac{\omega(x) - \omega_0}{\omega_1}\Big)\Big]. \qquad (2)$$

Here, λ is the modulation wave wavelength (λ = 2.8 nm for Rb_2ZnCl_4 [2]). This value is roughly equal to the c lattice constant in the C phase, which in turn is three times that in the P phase. We determined X_{max} at an NMR frequency that is $\sim$ 1 kHz away from the edge singularity. At this frequency, we obtained values for X_{max} in the range of (1.3±0.3) Å at 296.0 K and (2.4±0.3) Å at 301.6 K. This shows that at higher temperatures the modulation wave travels a greater distance, due to its higher mobility resulting from increased thermal depinning. However, these results contrast completely with results from the P phase (described in [16]). Figure 7, obtained at 326 K in the P phase, shows a *sudden* jump at a certain value for t_{mix}, after which it remains constant. This behavior clearly suggests that motions now occur only between two sites. This is confirmed by measurements of the ratio

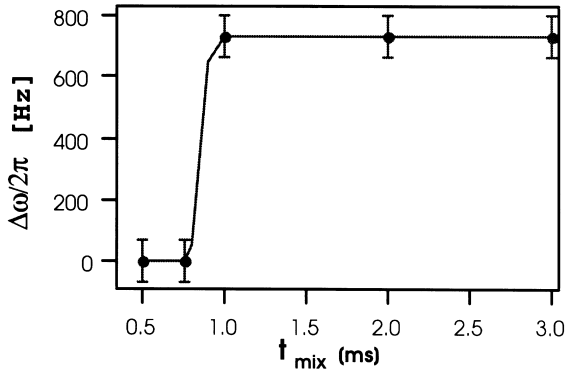

Fig. 7. The observed change in the NMR frequency, $\Delta\omega/2\pi$, due to motions plotted as a function of the mixing time, $t_{\rm mix}$, at T = 326 K. Reprinted with permission from [16].

of the cross to diagonal peak intensities $R(t_{\rm mix})$ in a standard 2D exchange spectrum vs. mixing time 16]. The slight discrepancy between our results and that in [14] ($X_{\rm max}$ = 1.58 Å at 291 K) likely reflects differences in impurity content (which probably varies slightly from sample to sample).

The possibility that either the P-phase or I-phase motions could reflect reorientations of only the $ZnCl_4^-$ groups without simultaneous Rb motions can be ruled out by the following consideration. According to Abragam [28], the second-order shift in the central (1/2 → –1/2) transition is given by

$$\omega_{1/2}^{(2)} = -\frac{\omega_Q^2}{16\omega_0}\left(a-\frac{3}{4}\right)\left(1-\mu^2\right)\left(9\mu^2-1\right), \quad (3)$$

where $a = I(I+1)$, $\mu = \cos\theta$, and $\omega_Q = \frac{3e^2qQ}{\hbar\cdot 2I(I-1)}$. θ is the angle that the external magnetic field $\vec{H}_0$ makes with a principal axis of the EFG tensor, and q is defined as V_{ZZ}/e, where V_{ZZ} is the largest principal component of the EFG tensor. Since V_{ZZ} depends on the distance of the field point from its source, (3) can be used to calculate the change in the second order shift due to a displacement of the charges responsible for the EFG. For a point charge, $V_{ZZ} \sim 1/r^3$. Substituting into (3), we obtain for small changes Δr in the distance from the point charge the following expression for the change in $\omega_{1/2}^{(2)}$:

$$\Delta\omega_{1/2}^{(2)} = K\frac{(eQV_{ZZ})^2}{\hbar^2\omega_0}\frac{\Delta r}{r}, \quad (4)$$

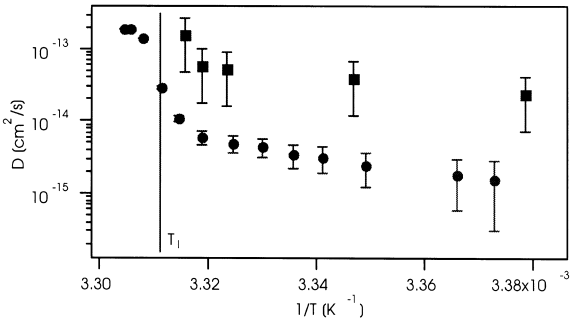

Fig. 8. The temperature variation of the diffusion coefficient obtained from ● ^{87}Rb Hahn spin-echo decay NMR and ■ ^{87}Rb 2D exchange-difference NMR.

where K is a numerical factor which, for our case (I = 3/2), has a maximum value (for θ = 90°) that is approximately equal to 0.3. In the P phase of Rb_2ZnCl_4, there exist two possible orientations of the $ZnCl_4$ tetrahedra that are occupied with equal probabilities [29 - 31]. Consider rotations of the $ZnCl_4$ tetrahedra between these two orientations. The distances separating the equilibrium positions of the Cl ions in these two orientations have been found by x-rays [31] to be between 0.22 Å and 0.48 Å for different Cl ions. Using these values and the value [22] e^2qQ/h = 3.75 MHz for Rb(2), we find that the maximum change in the ^{87}Rb NMR frequency due to $ZnCl_4$ reorientations is only approximately 15 Hz, which is far less than what is observed for the maximum cross peak displacement (700 Hz) (see Fig. 7). In the I phase the reorientational steps will be considerably smaller so that one can easily conclude that $ZnCl_4$ reorientations alone cannot account for our 2D ^{87}Rb observations either in the I or in the P phase. It is easy to see, however, that if the Rb ions are also slightly displaced (say by only 0.01 Å), the observed cross peak displacement can result.

We can estimate the value of the diffusion coefficient by using the formula

$$D = \frac{X_{\rm av}^2}{2\tau}. \quad (5)$$

This formula is valid for an isotropic, continuous medium. A rough value for τ in (5) can be estimated by equating it to the mixing time required to reach the maximum frequency change, $\Delta\omega_{\rm max}/2\pi$. Using this approach and (5), we estimated the diffusion coefficient at T = 301.6 K, in the high temperature region

of the I phase, to be $D = 1.4{\cdot}10^{-13}$ cm^2/s. As the temperature is lowered to $T = 296.0$ K, the value of D decreases to $D = 2.1{\cdot}10^{-14}$ cm^2/s. These values of D are of comparable order of magnitude with those obtained from ^{87}Rb NMR (see Fig. 8). The difference in the values of D obtained from the different experimental approaches is observed to increase at lower temperatures. This may be due to the possibility that the approximation of a continuous medium is probably not strictly valid at the lower temperatures (due to an increased effect of impurity pinning at the lower temperatures), in which case the use of (5) may not be adequate. Furthermore, the arbitrariness in determining τ described above could easily account for a factor of 2 or 3 in the value of D.

5. Summary

In this paper we used Hahn-echo and 2D exchange-difference NMR to investigate modulation wave motions in the incommensurate phase of Rb_2ZnCl_4. In particular, we have presented conclusive evidence for the existence of modulation wave diffusion in this system. This type of motion was earlier inferred in this system by a complementary experiment, the ^{35}Cl NQR Hahn spin-echo decay. However, a short Hahn spin-echo decay can in some systems be due to other possible motional mechanisms [32] that cannot be easily distinguished just by observation of a more rapid Hahn echo decay.

We measured ^{87}Rb NMR and ^{35}Cl NQR Hahn spin echo magnetization decays in the I phase of Rb_2ZnCl_4 and, in each case, obtained a Hahn echo decay that was shorter than the CPMG decay and one which decayed with a time constant proportional to the cube of the echo time. From these measurements we determined the diffusion coefficients and obtained similar values for ^{87}Rb NMR and ^{35}Cl NQR, a fact that strongly supports the existence in the I phase of slow modulation wave motion, since such motion should affect both Rb and Cl ions comparably. Furthermore, we have shown that our results can not be explained just by $ZnCl_4$ reorientations alone, but must also involve simultaneous motions of Rb atoms.

We also used ^{87}Rb 2D exchange-difference NMR to further confirm the existence of modulation wave diffusion in the incommensurate phase of Rb_2ZnCl_4. Our observation of a gradual increase in the cross-peak displacement vs. mixing time is evidence that the modulation wave is moving in steps that are small compared to its wavelength.

We estimated the diffusion coefficient of the modulation wave in the I phase of Rb_2ZnCl_4 by using all three experiments: ^{87}Rb NMR Hahn spin-echo decay, ^{35}Cl NQR Hahn spin-echo decay, and ^{87}Rb 2D exchange-difference NMR. The values of the diffusion coefficients are of comparable magnitude within experimental errors, especially in the high temperature region of the I phase, and this fact strongly supports the existence of the slow diffusion-like motion of the modulation wave.

Acknowledgements

This research was supported by the US NSF under Grant DMR-9624962. One of the authors (L. M.) was supported in part by a University of Utah Graduate Research Fellowship.

Appendix

Derivation of (2), the Relation Between the NMR Frequency Change and the Average Displacement of the Modulation Wave

The variation of the NMR or NQR frequency with position for a one dimensional modulation wave can be described in the linear case by

$$\omega(x) = \omega_0 + \omega_1 \sin(kx). \tag{A.1}$$

Assume that the modulation wave travels a distance Δx. Then the NMR frequency is

$$\omega(x + \Delta x) = \omega_0 + \omega_1 \sin\left[k(x + \Delta x)\right]). \tag{A.2}$$

The change in NMR frequency due to the motion of the modulation wave is then

$$\Delta\omega(x) = \omega(x + \Delta x) - \omega(x). \tag{A.3}$$

The distance Δx traveled by the modulation wave is then

$$\Delta x = \frac{1}{2\pi}\left[\arcsin\left(\frac{\omega(x + \Delta x) - \omega_0}{\omega_1}\right) - \arcsin\left(\frac{\omega(x) - \omega_0}{\omega_1}\right)\right]. \tag{A.4}$$

where $2\pi/\lambda = k$. The *maximum* modulation wave displacement $X_{\max}$ corresponds to a *maximum* change

in the NMR frequency $\Delta\omega_{\max}$. Using (A.3) and (A.4), we obtain for $X_{\max}$ the expression

$$X_{\max} = \frac{\lambda}{2\pi}\Big[\arcsin\Big(\frac{\Delta\omega_{\max} + \omega(x) - \omega_0}{\omega_1}\Big) - \arcsin\Big(\frac{\omega(x) - \omega_0}{\omega_1}\Big)\Big]. \quad \text{(A.5)}$$

[1] R. Blinc, Phys. Rep. **79**, 331 (1981).
[2] See "Incommensurate Phases in Dielectrics", edited by R. Blinc and A. P. Levanyuk, North-Holland, Amsterdam 1986, Vol. 1 and 2.
[3] R. Blinc, V. Rutar, B. Topič, F. Milia, I. P. Alexandrova, A. S. Chaves, and R. Gazzinelli, Phys. Rev. Lett. **46**, 1406 (1981).
[4] R. Blinc, P. Prelovšek, A. Levstic, and C. Filipič, Phys. Rev. B **29**, 1508 (1984).
[5] D. Michel, B. Muller, J. Peterson, A. Trumpert, and R. Walisch, Phys. Rev. B **43**, 7507 (1991).
[6] R. Blinc, S. Južnič, V. Rutar, J. Seliger, and S. Žumer, Phys. Rev. Lett. **44**, 609 (1980).
[7] R. Kind, J. Mol. Struct. **111**, 245 (1983).
[8] R. Blinc, F. Milia, V. Rutar, and S. Žumer, Phys. Rev. Lett. **48**, 47 (1982).
[9] K. P. Holzer, J. Petersson, D. Shubler, R. Walisch, U. Häcker, and D. Michel, Europhys. Lett. **31** (4), 213 (1995).
[10] P. Mischo, F. Deker, U. Häcker, K.-P. Holzer, J. Petersson, and D. Michel, Phys. Rev. Lett. **78**, 2152 (1997).
[11] D. C. Ailion and J. A. Norcross, Phys. Rev. Lett. **74**, 2383 (1995).
[12] G. Papavassiliou, M. Fardis, A. Leventis, F. Milia, and J. Dolinšek, Phys. Rev. Lett. **74**, 2387 (1995).
[13] G. Papavassiliou, M. Fardis, A. Leventis, F. Milia, J. Dolinšek, T. Apih, and M.-U. Mikac, Phys. Rev. B **55**, 12161 (1997).
[14] J. Dolinšek and G. Papavassiliou, Phys. Rev. B **55**, 8755 (1997).
[15] J. Dolinšek, B. Zalar, and R. Blinc, Phys. Rev. B **50**, 805 (1994).
[16] L. Muntean and D. C. Ailion, Phys. Rev. B **62**, 11 351 (2000).
[17] Y. Carr and E. M. Purcell, Phys. Rev. **94**, 630 (1954); S. Meiboom and D. Gill, Rev. Sci. Instrum. **29**, 6881 (1958).
[18] M. Takigawa and G. Saito, J Phys. Soc. Japan **55**, 1233 (1986).
[19] R. K. Subramanian, L. Muntean, J. Norcross, and D. C. Ailion, Phys. Rev. B **61**, 996 (2000).
[20] H. Z. Cummins, Phys. Rep. **185**, 211 (1990).
[21] M. Iizumi, J. D. Ace, G. Shirane, and K. Shimoaka, Phys. Rev. B **15**, 4392 (1977).
[22] V. Rutar, J. Seliger, B. Topic, R. Blinc, and I. P. Aleksandrova, Phys. Rev. B **24**, 2397 (1981).
[23] D. I. Hoult and R. E. Richards, F. R. S., Pros. Roy. Soc. Lond. A **344**, 311 (1975).
[24] R. R. Ernst, G. Bodenhausen, and A. Wokaunn, Principles of Nuclear Magnetic Resonance in One and Two Dimensions, Clarendon Press, Oxford 1987.
[25] L. Muntean, PhD thesis, University of Utah (2000), unpublished.
[26] J. Dolinšek, A. M. Fajdiga-Bulat, T. Apih, R. Blinc, and D.C. Ailion, Phys. Rev. B **50**, 9729 (1994).
[27] A. M. Fajdiga, T. Apih, J. Dolinšek, A. P. Levanyuk, S. A. Minyukov, and D. C. Ailion, Phys. Rev. Lett. **69**, 2721 (1992).
[28] A. Abragam, The Principles of Nuclear Magnetism, Clarendon Press, Oxford, 1961, p. 234.
[29] M. Quilichini and J. Pannetier, Acta Crystallogr. B **39**, 657 (1983).
[30] K. Itoh, A. Hinasada, M. Daiki, A. Ando, and E. Nakamura, Ferroelectrics **66**, 287 (1986).
[31] K. Itoh, A. Hinasada, H. Natasunga, and E. Nakamura, J. Phys. Soc. Japan. **52**, 664 (1983).
[32] D. W. Pfitsch, A. F. McDowell, and M. S. Conradi, J. Magn. Reson. **139**, 364 (1999).